A polarized view on DNA under tension

van Mameren, J.; Vermeulen, K.; Wuite, G.J.L.; Peterman, E.J.G.

DOI
10.1063/1.5004019
Publication date
2018
Document Version
Other version
Published in
Journal of Chemical Physics

Supplementary Information for:

A polarized view on DNA under tension

Joost van Mameren[1,2], Karen Vermeulen[1], Gijs J.L. Wuite[1] and Erwin J.G. Peterman[1]

1. Department of Physics and Astronomy and LaserLaB, Vrije Universiteit, Amsterdam, The Netherlands

2. Institute of Physics, University of Amsterdam, The Netherlands

Correspondence to Erwin J.G. Peterman e.j.g.peterman@vu.nl

1 Monte Carlo simulations of DNA with fixed ends

To interpret the shape of fluorescence intensity traces at DNA extensions up to the overstretching regime (i.e., $L/L_0 < 1$) we set out to simulate DNA conformations undergoing Brownian dynamics, while keeping the end points fixed: $L/L_0 = \text{constant}$. We employed the Metropolis scheme for Monte Carlo (MC) simulations[1, 2]. Using this algorithm, average values for observables of a system can be calculated by randomly sampling the phase space of those quantities. The efficiency of the algorithm relies on a smart selection for generating a next state to be sampled. Typically, a new state is generated by making a random change to the current state, a Monte Carlo 'move'. For this new state, the energy difference ΔE with the previous one is calculated. Any new state with $\Delta E<0$, i.e., with lower energy than the previous state, is 'accepted'. If $\Delta E > 0$, the new state is accepted with a probability equal to the Boltzmann factor: $\exp\left(-\frac{\Delta E}{k_B T}\right)$, where $k_B T$ is the thermal energy[1]. For accepted states, the relevant parameters are calculated to obtain an expectation value.

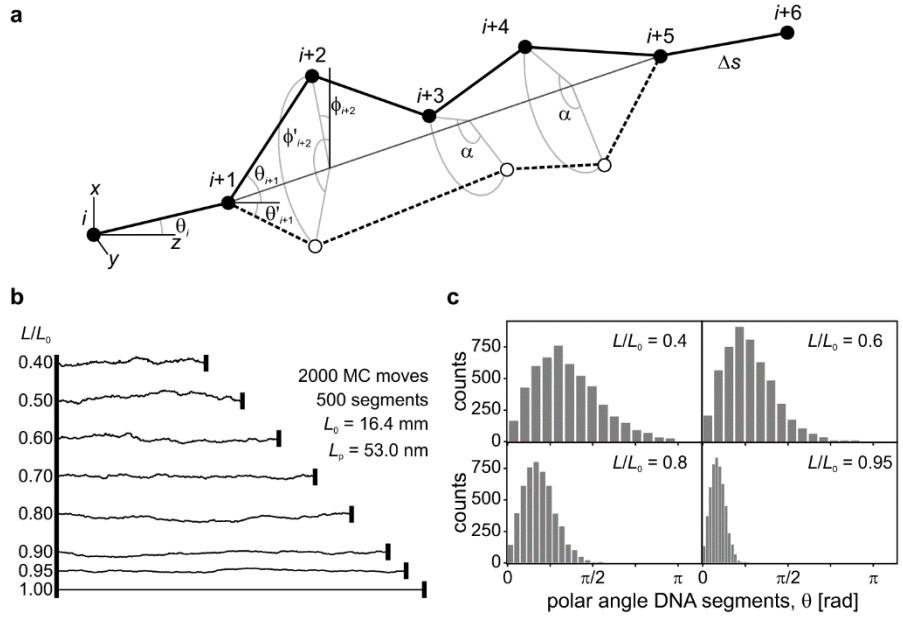

Supplementary Figure 1: **Monte Carlo simulations of extended DNA with fixed end points.** [**a**] Parametrization of a DNA molecule in segments with polar angles (θ_i, ϕ_i). The end points of the DNA lie along the *z*–axis. The Monte Carlo 'moves' are made by randomly selecting two nodes along the molecule, and rotating all segments in between these nodes around the line connecting them with a randomly selected angle α. [**b**] Simulated molecules for the fractional extensions L/L_0 indicated on the left. [**c**] Distributions of axial angles θ for four values of L/L_0, indicating the straightening out of the DNA. Azimuthal angles ϕ are uniformly distributed in all cases.

We simulated DNA molecules with a contour length L_0 as chains of N rigid segments of length $\Delta s = L_0/N$, with axial angle θ_i with respect to the laboratory *z*–axis and an azimuthal axis ϕ_i around it (Supplementary Figure 1a). For a given contour length L_0, a starting configuration with end-to-end length L was generated by setting $\phi_i = 0$, and $\theta_i = \arccos(L/L_0)$ for $0 < i < N/2 - 1$ and $\theta_i = -\arccos(L/L_0)$ for $N/2 < i < N - 1$, i.e., a triangle. Alternatively, the starting configuration could be set to alternating positive and negative angles

$|\theta_i| = \arccos(L/L_0)$, i.e., a zig-zag pattern. The Monte Carlo moves were performed as follows. Two nodes along the molecule's contour were randomly selected (e.g., i+1 and i+5 in Supplementary Figure 1a). All segments in between these nodes where then rotated around the line connecting the nodes by a random angle $\alpha \in [0,2\pi]$ (Supplementary Figure 1a). The energy of both states was calculated from the bending energy:

$$E = \frac{L_p k_B T}{2} \int_0^L \left(\frac{d\xi}{ds}\right)^2 ds = \frac{L_p k_B T}{2\Delta s} \sum_{i=0}^{N-1} \Delta\xi_i^2, \quad \text{(S1)}$$

where L_p is the persistence length of the DNA, Δs the length of a segment and $\Delta\xi_i$ the angle between segments i and i+1, obtained using the inner product. In practice, only the energy change at the (randomly) selected nodes was calculated to reduce computational costs.

This choice of MC moves ensures an efficient sampling of phase space because of its delocalized nature, while keeping the end-to-end distance unchanged. Typically, the number of MC moves required to avoid 'memory' of the artificial starting configuration was $\sim 3-5N$. This equilibration was seen as the total energy of the molecule leveling off to reach a steady state. This was found to be independent of which starting configuration was used: the low-energy triangle state with a single bend or the high-energy zig-zag state.

Supplementary Figure 1b shows molecules at the indicated end-to-end distances L/L_0, simulated using the parameters indicated on the right. Using the simulations, distributions of polar coordinates θ and ϕ were obtained as a function of L/L_0. For all values of L/L_0, distributions of azimuthal angles ϕ are uniform between 0 and 2π. Supplementary Figure 1c shows the distributions of axial angles θ for four values of L/L_0, and how the distributions narrow when the molecules are stretched. The vanishing of θ near 0 is due to the fact that the density of polar coordinate states vanishes at $\theta = 0$: $d\Omega = \sin\theta d\theta d\phi$.

The simulations were used to calculate expectation values for the polarized fluorescence intensities in the DNA stretching experiments, as discussed in the next sections.

2 Dye mobility induced by DNA dynamics: 'slow wobble'

Irving[3] developed a framework to calculate the observable quantities, ${}_{\parallel}I_{\parallel}$, ${}_{\perp}I_{\parallel}$, ${}_{\parallel}I_{\perp}$, ${}_{\perp}I_{\perp}$, in terms of the polar orientation angles of a fluorescent dye with its absorption and emission dipoles cylindrically distributed around the *z*–axis. Here, we repeat those equations from his work that are required for a proper understanding of our approach. Irving calculated the probabilities $p_{\parallel}, p_{\perp}$ of absorbing and emitting light with its polarization parallel or perpendicular to the *z*–axis. These probabilities being equal to the squared projection of the dipole vector onto the respective axes, this yields[3] :

$$\text{fixed dye} \begin{cases} {}_{\parallel}I_{\parallel} = k\cos^2\theta_a \ \cos^2\theta_e\,, \\ {}_{\parallel}I_{\perp} = k\cos^2\theta_a \ \sin^2\theta_e\cos^2\phi_e\,, \\ {}_{\perp}I_{\parallel} = k\sin^2\theta_a \ \cos^2\theta_e \ \cos^2\phi_a\,, \\ {}_{\perp}I_{\perp} = k\sin^2\theta_a \ \sin^2\theta_e \ \cos^2\phi_a \ \cos^2\phi_e\,, \end{cases} \tag{S2}$$

with θ_a and θ_e the polar angles of respectively the absorption and emission dipole moments with respect to the z–axis, ϕ_a and ϕ_e the corresponding azimuthal angles and k a normalization constant. In practice, absorption and emission dipoles intercalating dyes chromophores[4].

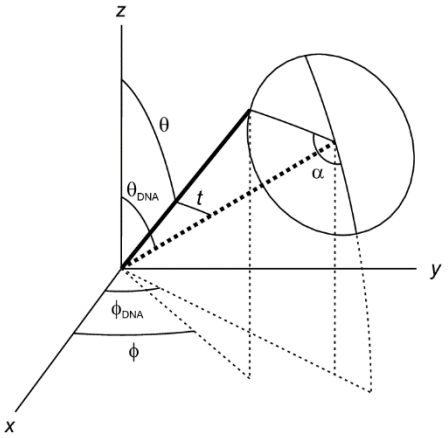

Supplementary Figure 2: **Angular coordinates for a dye with static inclination with respect to a symmetry axis.** The (absorption or emission) dipole moment of a dye (thick solid line) makes axial and azimuthal angles t and α with its symmetry axis with polar coordinates $(\theta_{DNA}, \phi_{DNA})$ (thick dashed line). The dipole's coordinates (θ, ϕ) can be expressed in terms of the parametric coordinates (t, α) and the symmetry axis coordinates using the spherical law of cosines (equation S3).

To interpret the measured polarized fluorescence intensities at DNA extensions below the overstretching regime $(L/L_0 < 1)$ and account for 'slow wobble' dynamics, we set out to calculate expectation values for ${}_{ex}I_{em}$ from the simulated molecules described in the Supplementary Method 1, for a dye with cylindrical symmetry not around one of the laboratory axes, but around the axis of a simulated DNA segment with polar angles $(\theta_{DNA}, \phi_{DNA})$. The dipole axis makes an angle *t* with this DNA segment; its azimuthal angle α is measured with respect to the plane defined by the *z*–axis and that of the DNA. Supplementary Figure 2 gives a graphical

definition of these parameters. We rewrite equations S2 in terms of these new parameters, making use of the spherical law of cosines and a derivative of it[3]:

$$\cos\theta = \cos t \cos\theta_{DNA} - \sin t \sin\theta_{DNA}\cos\alpha,$$
$$\sin\theta\cos\phi = \cos t \sin\theta_{DNA}\cos\phi_{DNA} + \sin t \cos\alpha\cos\theta_{DNA}\cos\phi_{DNA} - \sin t \sin\alpha \sin\phi_{DNA}. \quad \text{(S3)}$$

Substituting equations S3 into equations S2 and integrating over α around the symmetry axis, we find for ${}_{\parallel}I_{\parallel}$ (assuming parallel absorption and emission dipoles):

$$\begin{aligned} {}_{\parallel}I_{\parallel} = {} & 4\big(44\cos 2t + 5(\cos 4t + 3)\big)\cos 2\theta_{DNA} \\ & + (20\cos 2t + 35\cos 4t + 9)\cos 4\theta_{DNA} \\ & 60\cos 2t + 9\cos 4t + 123. \end{aligned} \quad \text{(S4)}$$

Similar (but significantly more complex) equations are obtained for ${}_{\perp}I_{\parallel}$, ${}_{\parallel}I_{\perp}$, ${}_{\perp}I_{\perp}$. Using these equations, the observable quantities ${}_{ex}I_{em}$ and the P and Q polarization ratios can be analytically calculated for Monte Carlo simulated DNA molecules at any fractional extension. By averaging these quantities over large numbers of simulated DNA conformations, we calculate the effect of slow-wobble dynamics.

3 Dye mobility on the fluorescence time scale: 'fast wobble'

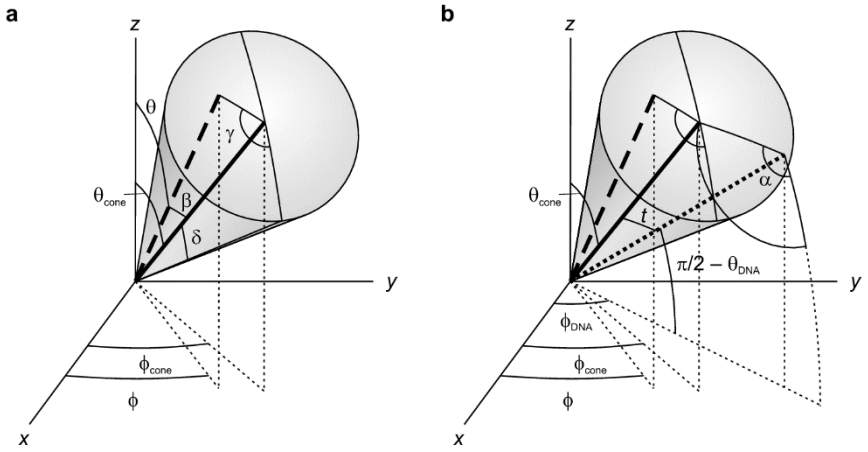

Supplementary Figure 3: **Angular coordinates for a dye undergoing rapid motion in a cone.** [**a**] The cone axis (thick solid line) is defined by polar angles $(\theta_{cone}, \phi_{cone})$. A dipole vector in the cone (thick dashed line), defined by polar angles (θ, ϕ) is parametrized by azimuthal angle γ and axial angle β (running from 0 to δ, the semi-angle of the cone). [**b**] Like in Figure S2, the cone axis coordinates can be expressed in terms of the angular distance to a DNA segment axis with coordinates $(\theta_{DNA}, \phi_{DNA})$ (thick dotted line).

Irving expanded his calculations to account for rapid motion of the dye on the time scale of fluorescence absorption and emission, 'fast wobble'[3]. Assuming the dye to diffuse freely in a cone of semi-angle δ, the general polarized intensity ${}_{ex}I_{em}$ is given by:

$$ {}_{ex}I_{em} = \frac{\iint p_{am}(\theta_a,\phi_a)d\Omega \iint p_{en}(\theta_e,\phi_e)d\Omega}{(\iint d\Omega)^2}, \tag{S5} $$

where the integrals are taken over the solid angle of the cone:

$$ \iint d\Omega = \int_{\gamma=0}^{2\pi}\int_{\beta=0}^{\delta} \sin t \, d\beta \, d\gamma = 2\pi(1-\cos\delta), \tag{S6} $$

with γ and β the parametric coordinates of a dipole vector in the cone (see Figure S3a). Using equations S3, the integrals of the absorption probabilities p_{am} and p_{en} in equation S5 can be explicitly calculated, yielding[3]:

$$ \iint p_{a\parallel}(\theta_a,\phi_a)d\Omega = 2\pi(1-\cos\delta)\left(\frac{k}{2}\right)\left[\omega + (2-3\omega)\sin^2\theta_{cone,a}\right], \tag{S7} $$

$$ \iint p_{a\perp}(\theta_a,\phi_a)d\Omega = 2\pi(1-\cos\delta)\left(\frac{k}{2}\right)\left[\omega + (2-3\omega)\sin^2\theta_{cone,a}\cos^2\phi_{cone,a}\right], \tag{S8} $$

$$ \text{with } \omega = 1-(1+\cos\delta+\cos^2\delta)/3. \tag{S9} $$

The emission probabilities are obtained simply by substituting suffixes 'a' by 'e'. In Irving's derivation, the result of the above integrations was integrated over the azimuthal angle ϕ to account for the rotational symmetry around the z–axis. In our case of rotational symmetry around a DNA segment with coordinates $(\theta_{DNA}, \phi_{DNA})$,

we need to integrate around this segment's axis. We therefore parametrize our coordinates again in terms of this axis with the quantities introduced in Figure S3b using the spherical cosine law once more (Eq. S3). The resulting polarized intensities read:

$$
\begin{aligned}
{}_{\parallel}I_{\parallel} = k \int_0^{2\pi} d\alpha [\omega + (2-3\omega)[\cos t \cos\theta_{DNA} - \cos\alpha \sin t \sin\theta_{DNA}]^2] \\
\times [\omega + (2-3\omega)[\cos t \cos\theta_{DNA} - \cos(\alpha-\beta) \sin t \sin\theta_{DNA}]^2],
\end{aligned} \tag{S10}
$$

$$
\begin{aligned}
{}_{\parallel}I_{\perp} = k \int_0^{2\pi} d\alpha [\omega + (2-3\omega)[\cos t \cos\theta_{DNA} - \cos\alpha \sin t \sin\theta_{DNA}]^2] \\
\times [\omega + (2-3\omega)[\cos\phi_{DNA} (\cos(\alpha-\beta) \sin t \cos\theta_{DNA} \\
+ \cos t \sin\theta_{DNA}) - \sin t \sin(\alpha-\beta) \sin\phi_{DNA}]^2],
\end{aligned} \tag{S11}
$$

$$
\begin{aligned}
{}_{\perp}I_{\parallel} = k \int_0^{2\pi} d\alpha [\omega + (2-3\omega)[\cos t \cos\theta_{DNA} - \cos(\alpha-\beta) \sin t \sin\theta_{DNA}]^2] \\
\times [\omega + (2-3\omega) [\cos\phi_{DNA} (\cos\alpha \cos\theta_{DNA} \sin t + \cos t \sin\theta_{DNA}) \\
- \sin t \sin\alpha \sin\phi_{DNA}]^2],
\end{aligned} \tag{S12}
$$

$$
\begin{aligned}
{}_{\perp}I_{\perp} = k \int_0^{2\pi} d\alpha [\, \omega + (2-3\omega)[\cos\phi_{DNA} (\cos\alpha \sin t \cos\theta_{DNA} + \cos t \sin\theta_{DNA}) \\
- \sin\alpha \sin t \sin\phi_{DNA}]^2] \times [\, \omega + (2-3\omega)[\cos\phi_{DNA} \\
\times (\cos(\alpha-\beta) \sin t \cos\theta_{DNA} + \cos t \sin\theta_{DNA}) \\
- \sin(\alpha-\beta) \sin t \sin\phi_{DNA}]^2],
\end{aligned} \tag{S13}
$$

Here we have assumed that $\theta_a = \theta_e$. We have written $\beta = \phi_a - \phi_e$ for the azimuthal angle difference between absorption and emission dipoles. This parameter can be used to account for energy transfer between the two dye moieties of a bis-intercalating dye. In that case, the azimuthal angle difference between the dyes, depending on their axial distance and the helical pitch of DNA[5], will set the angle difference between the absorbing and emitting dipole, as discussed in the Materials and Methods section of the main text.

The integrals over α can in principle be calculated analytically. However, the mathematical complexity is such that numerical evaluation is more efficient. Doing so, we can simultaneously take into account the depolarizing effects of slow-wobble and fast-wobble dynamics.

4 Transmission and high-NA corrections

The transmission of the microscope optics for the two orthogonal polarizations need not be equal *a priori*. Particularly dichroic mirrors, placed under 45°, display unequal polarized transmissions[6]. Therefore, we measured the transmission of the excitation laser after the microscope objective using a power meter—found as a ratio of 1.12—and corrected for the consequent difference in excitation power between the two orthogonal polarizations. Likewise, we determined the transmission ratio *M* of the two fluorescence polarizations from the sample to the camera. We hereto measured the anisotropy of a homogeneous sample of YOYO-labeled DNA molecules with two orthogonal excitation polarizations:

$$r_1 = \frac{{}_{\parallel}I_{\parallel} - M\ {}_{\parallel}I_{\perp}}{{}_{\parallel}I_{\parallel} + 2M\ {}_{\parallel}I_{\perp}}, \tag{S14}$$

$$r_1 = \frac{M\ {}_{\perp}I_{\perp} - {}_{\perp}I_{\parallel}}{M\ {}_{\perp}I_{\perp} + 2\ {}_{\perp}I_{\parallel}}, \tag{S15}$$

Since the anisotropy is a property of the sample, independent of the microscope optics, r_1 and r_2 should be equal, and can thus be used to find the ratio *M*, yielding a value of 0.68.

A last correction was required to compensate for the high numerical aperture (NA) of the water-immersion objective of NA=1.2. This high NA results in partial depolarization of high-angle (i.e., off-axis) emitted fluorescence, causing mixing between the observed intensities ${}_{ex}I_{em}$. Axelrod derived expressions for this correction[7, 8]. An emitting dipole in the sample that has intensity components $\left(I_x = I_\perp,\ I_y = I_\parallel,\ I_z = I_\perp\right)$ (Figure 3) when observed at low NA, will be observed as:

$$(I_\perp)_{\text{observed}} = c_1 I_x + c_3 I_y + c_2 I_z, \tag{S16}$$

$$(I_\parallel)_{\text{observed}} = c_1 I_x + c_2 I_y + c_3 I_z, \tag{S17}$$

Axelrod analytically derived the coefficients c_1, c_2 and c_3 to be[7, 8]:

$$c_1 = \frac{2 - 3\cos\sigma + \cos^3\sigma}{6(1 - \cos\sigma)}, \tag{S18}$$

$$c_2 = \frac{1 - 3\cos\sigma + 3\cos^2\sigma - \cos^3\sigma}{24(1 - \cos\sigma)}, \tag{S19}$$

$$c_3 = \frac{5 - 3\cos\sigma - \cos^2\sigma - \cos^3\sigma}{8(1 - \cos\sigma)}, \tag{S20}$$

Here, σ is the maximum viewing angle of the objective: $\sigma = \arcsin(NA/n)$, with n being the refractive index of the immersion medium. For our water-immersion objective (n=1.33) of NA=1.2, these coefficients take on the values 0.23, 0.013, and 0.76, respectively. The observed polarized intensities ${}_{ex}I_{em}$ were corrected for this

mixing.

Supplementary figure 4

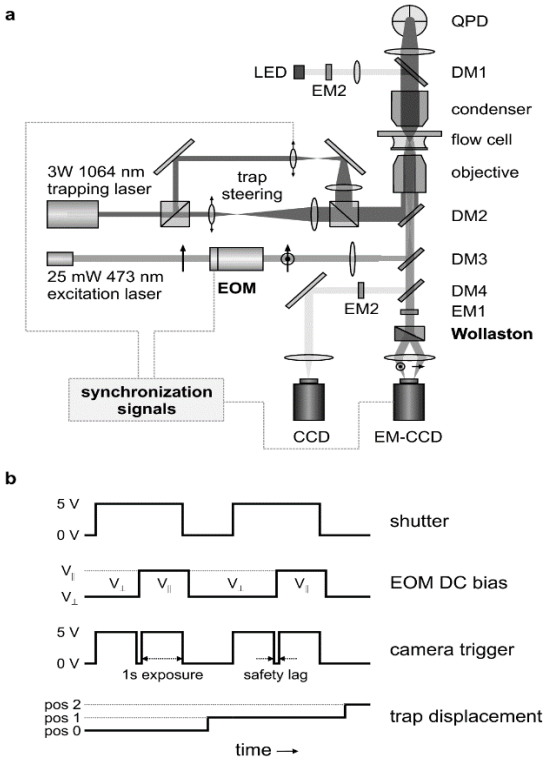

Supplementary Figure 4: **Experimental setup.** [**a**] Schematic of the combined dual trap and polarized fluorescence microscope. Abbreviations: EOM – electro-optic modulator; DM – dichroic mirror; EM – emission filter; QPD – quadrant photodiode; LED – light emitting diode; (EM-)CCD – (electron-multiplied) charge coupled device. [**b**] Synchronization signals (dashed lines in panel a) used for coordinated camera exposure, adjustment of excitation polarization, and trap displacement. The excitation polarization is alternated using a 2-step block signal supplied to the DC bias input of an electro-optic modulator. The polarization change occurs during the safety lag in between two camera exposures to avoid fluorescence recording with mixed polarizations.

Supplementary References

[1] D. Frenkel, and B. Smit, *Understanding Molecular Simulation* (Academic Press, Boston, 2002),
[2] N. Metropolis, A. W. Rosenbluth, M. N. Rosenbluth, A. H. Teller, and E. Teller, Journal of Chemical Physics **21** (1953) 1087.
[3] M. Irving, Biophys J **70** (1996) 1830.
[4] C. Carlsson, A. Larsson, M. Jonsson, B. Albinsson, and B. Norden, Journal of Physical Chemistry **98** (1994) 10313.
[5] C. Carlsson, A. Larsson, M. Bjorkman, M. Jonsson, and B. Albinsson, Biopolymers **41** (1997) 481.
[6] E. Hecht, *Optics* (Addison-Wesley, Reading, Mass., 1998), 3rd edn.,
[7] D. Axelrod, Biophys J **26** (1979) 557.
[8] D. Axelrod, Methods in Cell Biology **30** (1989) 333.